BIOCHEMISTRY
including biophysical chemistry & molecular biology
Article

Biochemistry **2009,** *48,* 7209–7218 7209
DOI: 10.1021/bi9007353

Size Limitation in Translocation of Fibroblast Growth Factor 1 Fusion Proteins across the Endosomal Membrane†

Malgorzata Zakrzewska,[‡,§] Yan Zhen,[‡,∥] Antoni Wiedlocha,[‡] Sjur Olsnes,[‡] and Jørgen Wesche*[,‡]

[‡]*Centre for Cancer Biomedicine, Faculty Division Norwegian Radium Hospital, University of Oslo, and Department of Biochemistry, Institute for Cancer Research, The Norwegian Radium Hospital, Montebello, 0310 Oslo, Norway,* [§]*Faculty of Biotechnology, University of Wroclaw, Tamka 2, 50-137 Wroclaw, Poland, and* [∥]*Department of Education and Science, First People's Hospital of YunNan Province, China*

Received April 29, 2009; Revised Manuscript Received June 26, 2009

ABSTRACT: After binding to its receptor on the surface of mammalian cells and subsequent endocytosis, FGF1 is translocated across the membrane into the cytosol. The growth factor is then further transported into the nucleus. In order to characterize more closely the translocation mechanism utilized by FGF1, we introduced additional amino acids into FGF1 to test the size dependence of the translocated substrate. We constructed mutants containing an increasing number of copies of the myc tag (1−13 copies) in a surface loop of the FGF1 molecule. All of the constructs bound to specific FGF receptors and to heparin and were taken up by endocytosis. However, only FGF1 mutants harboring up to three myc tags (53 amino acids) were translocated while mutants with five myc tags (77 amino acids) or more were not translocated through the membrane. We further showed that insertion of other, unrelated polypeptides into FGF1, i.e., 3×FLAG tag (22 amino acids) and streptavidin binding peptide (50 amino acids), was also translocated. Larger insertions into FGF1, like the CBP-SBP tag (82 amino acids) or ricin A-chain (272 amino acids), resulted in fusion proteins that failed to translocate. The presented data imply that it is possible to employ FGF1 to import various polypeptides into the cytosol and nucleus of cells. Furthermore, the strict size dependence of FGF1 fusion proteins in membrane translocation argues against simple leakage of FGF1 from ruptured endosomal membranes but rather points to a specific translocation apparatus involving a proteinaceous pore.

FGF1 binds to specific transmembrane tyrosine kinase receptors (FGFRs)[1] at the surface of target cells. The binding causes dimerization and activation of the FGF receptors initiating downstream signaling cascades such as the Ras/MAPK, PI-3 kinase, and PLCγ pathways (*1*). After binding, the FGF/FGFR complex is taken up into the cell by endocytosis leading to downregulation of the tyrosine kinase signaling (*2*, *3*). In addition to activating the tyrosine kinase receptor, FGF1 has the unusual ability to translocate across the endosomal membrane into the cytosol and then to be further transported to the nucleus (*4*, *5*). Several intracellular proteins, e.g., CK2, FIBP, and Lrrc59 (formerly designated ribosome-binding p34), have been reported to interact with FGF1, and they may be involved in an intracellular signaling pathway (*6*−*8*). Some reports indicate that FGF1 localized to the nucleus may be involved in the regulation of DNA synthesis (*4*, *5*, *7*).

We characterized in some detail the pathway utilized by externally added FGF1 to reach the nucleus. FGF1 translocates into many of the mammalian cell types tested (NIH/3T3, BJ, U2OS, Hela, HUVEC, CPAE, and COS cells) (*9*−*13*). There seems to be a requirement for serum starvation of the cells for efficient translocation to occur (*14*). The translocation is a relatively slow process as added FGF1 appears first after 3−4 h in the nucleus (*14*). Then the level of FGF1 in the nucleus slowly increases and reaches a maximum after 6 h. The timing of FGF1 translocation into the nucleus coincides with the later part of the G1 phase of the cell cycle (*14*, *15*).

We showed that binding of FGF1 to specific high-affinity FGFRs is necessary for translocation (*10*, *16*). Interestingly, only FGFR1 and FGFR4 can mediate translocation while FGFR2 and FGFR3 do not have this property (*10*). Subsequent analysis revealed certain important amino acids in the C-terminal tail of the receptors which are crucial for translocation of the ligand FGF1 (*10*).

We found that the vesicular membrane potential is required for translocation, indicating that the translocation occurs from intracellular vesicles/endosomes (*11*, *14*). Furthermore, we provided evidence that the cytosolic chaperone Hsp90 is involved in translocation (*17*). Both the membrane potential and the chaperone may provide the energy necessary for the translocation of FGF1 across the membrane. Similarly to translocation of proteins into peroxisomes, extensive unfolding appears not to be necessary for membrane translocation of FGF1 (*18*).

Importantly, the translocation seems to be tightly regulated by several signal transduction pathways. Cells treated with inhibitors against PI-3 kinase or p38 MAPK do not translocate FGF1 (*9*, *19*). The regulation by p38 MAPK was shown to involve the phosphorylation of FGFR1 on serine 777 (*9*).

†The work of M.Z. was supported by the Polish Ministry of Science and Higher Education (Grant N N301 4192 33). M.Z. is a Fellow of the Research Council of Norway. Y.Z. and J.W. are Fellows of the Norwegian Cancer Society.

*Corresponding author. Tel: +47 22934293. Fax: +47 22508692. E-mail: jorgen.wesche@rr-research.no.

[1]Abbreviations: FGF1, fibroblast growth factor 1; FGFR, fibroblast growth factor receptor; SDS−PAGE, sodium dodecyl sulfate−polyacrylamide gel electrophoresis; CD, circular dichroism; GdmCl, guanidinium chloride.

Published on Web 06/26/2009

After translocation across the endosomal membrane, FGF1 which contains two nuclear localization signals is transported into the nucleus (*12*). There, FGF1 is phosphorylated by PKCδ and transported out again by a nuclear export signal and then degraded (*20*, *21*).

Other proteins may use a similar system as FGF1 for translocation into cells. Several groups have reported that FGF2, a homologue of FGF1, is translocated across the membrane and transported into the nucleus (*14*, *22*−*25*). We provided evidence that the translocation route of FGF2 is identical to the one FGF1 uses (*14*). The HIV protein TAT was also reported to be translocated into the cell from endosomes and shows some similarities to the FGF1 translocation system (*26*, *27*). However, further experiments are needed to test if they use exactly the same mechanism. It is an interesting possibility that the translocation pathway characterized by FGF1 could be a general system used by several extracellular proteins for translocation into the cytosol.

In order to investigate the role of substrate size in the FGF1 translocation pathway, we constructed FGF1 mutants where we added polypeptides of different lengths into a loop in the FGF1 molecule. Using multiple copies of the myc tag and other polypeptides, we were able to construct mutants with different sizes. These mutants were used to test if size matters in the translocation process and then to probe the size-exclusion limit for FGF1 translocation.

EXPERIMENTAL PROCEDURES

Materials, Media, and Buffers. [*methyl*-^{3}H]Thymidine (25 Ci/mmol) was obtained from Amersham Biosciences. The basic components of culture media were supplied by Merck (Germany). Other chemicals were from Sigma. HEPES medium: bicarbonate- and serum-free Eagle's minimal essential medium buffered with 20 mM HEPES to pH 7.4. Lysis buffer: 0.1 M NaCl, 20 mM NaH_2PO_4, 10 mM EDTA, 1% Triton X-100, 1 mM PMSF, and 1 mM NEM, pH 7.4. PBS: 140 mM NaCl and 10 mM NaH_2PO_4, pH 7.4.

Site-Directed Mutagenesis and Plasmid Constructions. The coding sequence of FGF1 was amplified by PCR from the plasmid pB-FGF1 and cloned into pET21d to yield the plasmid pET21-FGF1. We inserted one copy of the myc tag (EQKLISEEDL) and the 3×FLAG tag (DYKDHDGDYKDHDIDYKDDDDK) into FGF1 (between the amino acids valine 51 and glycine 52 in the FGF1 sequence, using the numbering system introduced by Gimenez-Gallego et al. (*28*)) by QuikChange site-directed mutagenesis (Stratagene). To construct the other fusion protein vectors, we first introduced a linker between amino acids valine 51 and glycine 52 containing a sequence for the restriction sites *Eco*RI and *Sal*I to construct the vector pET-FGF-POLY. Introduction of the linker added five amino acids to the different insertions. The different number of myc tags was amplified from the vector pFA6a-13myc-kanMX6 (a kind gift from Dr. Beata Grallert) and introduced into the plasmid pET-FGF1-POLY cut with *Eco*RI and *Sal*I. We then obtained the following plasmids: pET-FGF1-myc2, -myc3, -myc4, -myc5, -myc8, and -myc13. To obtain a FGF1-myc5 variant with increased thermodynamic stability (stable FGF1-myc5, FGF1-myc5st), we introduced three previously described FGF1 stabilizing mutations, Q40P, S47I, and H93G, into the FGF1-myc5 construct using QuikChange multisite-directed mutagenesis (Stratagene) (*29*). The plasmid pET-FGF1-SBP was made by amplifying a fragment coding for the streptavidin binding peptide (MDEKTTGWRGGHVVEGLAGELEQLRARLEHHPQGQREPSGGCKLG) from the plasmid pNTAP (Stratagene) that was cloned into pET-FGF1-POLY cut with *Eco*RI and *Sal*I. The plasmid pET-FGF1-CBP-SBP was made by amplifying a fragment coding for both the calmodulin binding peptide (KRRWKKNFIAVSAANRFKKISSSGAL) and streptavidin binding peptide from the plasmid pNTAP (Stratagene) that was cloned into pET-FGF1-POLY cut with *Eco*RI and *Sal*I. The plasmid pET-FGF1-RTA was made by amplifying a sequence coding for ricin A-chain that was cloned into pET-FGF1-POLY cut with *Eco*RI and *Sal*I.

Expression and Purification of Recombinant Proteins. Expression of recombinant protein from the plasmids pET-FGF1, pET-FGF1-myc1, pET-FGF1-myc2, pET-FGF1-myc3, pET-FGF1-myc4, pET-FGF1-myc5, pET-FGF1-myc8, pET-FGF1-myc13, pET-FGF1-SBP, pET-FGF1-3×FLAG, pET-FGF1-CBP-SBP, and pET-FGF1-RTA in *Escherichia coli* BL21DE was induced with 1 mM isopropyl β-D-thiogalactopyranoside. The bacterial pellet was resuspended in 20 mM Na_2HPO_4, pH 7.5, 0.5 M NaCl, 1 mM dithiothreitol, and 1 mM EDTA and sonicated. The bacterial suspension was centrifuged at 20000*g* for 10 min at 4 °C, and then the supernatant was applied to a heparin−Sepharose column (Amersham Pharmacia). The bound material was washed with 0.7 M NaCl and then eluted with 2 M NaCl in 20 mM Na_2HPO_4, pH 7.4, 1 mM dithiothreitol, and 1 mM EDTA. For thermodynamic studies purified proteins were dialyzed into 25 mM phosphate buffer, pH 7.3.

Spectroscopic Studies. To analyze secondary and tertiary structure of recombinant FGF1 mutants, circular dichroism (CD) and fluorescence spectra at 19 °C were acquired. The CD spectra were collected in the 200−260 nm wavelength range on a spectropolarimeter with a response time of 1 s. Fluorescence measurements were performed using a spectrofluorometer with an excitation wavelength of 280 nm and emission spectra with a range from 300 to 450 nm. The measurements were performed at a protein concentration of 2 μM in 25 mM sodium phosphate buffer, pH 7.3, in cuvettes of 10 mm path length.

Circular dichroism and fluorescence measurements were also used to study thermodynamic stability of FGF1 variants. Thermal denaturations were performed in 25 mM phosphate buffer (pH 7.3) in the presence of 0.7 M guanidinium chloride (GdmCl), which prevents protein aggregation and accumulation of folding intermediates during the heating and ensure a two-state process (*29*−*31*). The temperature-induced ellipticity (CD) changes were followed at 227 nm in 10 mm path-length cuvettes using 8 s response time. Denaturation was performed in the spectrofluorometer and was monitored by changes in the emission signal at 353 nm of the single tryptophan residue excited at 280 nm (*28*). The measurements were carried out at a protein concentration of 2 μM. The data were analyzed assuming a two-state reversible equilibrium transition as described previously (*29*, *31*).

To analyze the ability of heparin to bind and protect FGF1 mutants against thermal unfolding, we performed the denaturation experiment using the CD technique in the absence and presence of a 5-fold molar excess of heparin. The measurements were carried out in the presence of 1.5 M urea (equivalent of 0.7 M GdmCl), which is a nonionic denaturant and does not disturb ionic interactions.

Laser Scanning Confocal Microscopy. U2OS cells stably expressing FGFR1 were grown on coverslips in tissue culture plates. FGF1 myc mutants were added together with heparin (50 units/mL), and the cells were incubated for 15 min. The cells

were fixed with methanol and incubated with anti-myc antibody from Abcam (rabbit) and anti-EEA1 (mouse) antibody from BD Transduction Laboratories. The cells were further incubated with appropriate secondary antibodies labeled with Cy3 and Cy2 Alexa488 (Jackson ImmunoResearch). The nucleus was stained with Hoechst 33342 from Invitrogen. The cells were then examined with a Zeiss LSM 510 META confocal microscope. Montages of images were prepared with the use of Adobe Photoshop 7.0.

Measurement of DNA Synthesis. Cells growing in 24-well tissue culture plates (5×10^4 cells per well) were preincubated for 24 h in 1.0% insulin−transferrin supplemented medium at 37 °C. Then the cells were treated with increasing concentrations of FGF1 or FGF1 mutants (0.1−100 ng/mL corresponding to 6.5 pM−6.5 nM) in the presence of 20 units/mL heparin, and the incubation was continued for 24 h more at 37 °C. During the last 6 h the cells were incubated with 1 μCi/mL [*methyl*-^{3}H]thymidine as described previously, and the incorporated radioactivity was measured (*4*).

FGF1 Signaling Assay. Cells were serum-starved for 24 h in DMEM. Then cells were treated with 20 units/mL heparin and 6.5 nM FGF1 or FGF1 mutants for 15 min, lysed in SDS sample buffer, and analyzed by SDS−PAGE and Western blotting using anti-phospho antibodies against signaling molecules activated by FGF1 stimulation. The following primary antibodies were used: mouse anti-phospho-FGFR, rabbit anti-phospho-FRS2-α, rabbit anti-phospho-Akt, rabbit anti-MAP kinase (p42/p44), mouse anti-phospho-MAP kinase (p42/p44) from Cell Signaling Technology, rabbit anti-phospho-PLCγ from Santa Cruz Biotechnology, mouse anti-phospho-p38 MAPK, and mouse anti-Hsp90 from BD Transduction Laboratories.

Fractionation of BJ and NIH/3T3 Cells. For fractionation, BJ or NIH/3T3 cells were incubated with FGF1 or FGF1 mutants (100 ng/mL, i.e., 6.5 nM) in the presence of 20 units/mL heparin for 6 h at 37 °C and washed with high salt/low pH buffer (2 M NaCl in 20 mM sodium acetate, pH 4.0). The cells were then washed with PBS, and 20 μg/mL digitonin was added to permeabilize the cells. After 5 min incubation at 25 °C, the cells were kept on ice for additional 30 min to allow components of the cytosol to diffuse into the buffer. The medium was recovered and denoted the cytosolic fraction. The remainder of the cells were lysed with lysis buffer and scraped from the plastic to recover nuclei and centrifuged at 15800*g* for 15 min. The supernatant was designated the membrane fraction. The pellet was washed three times in lysis buffer. After sonicating for 10 s on ice, the lysate was centrifuged for 5 min at 15800*g*, and the supernatant was designated the nuclear fraction. The different fractions were adsorbed to heparin−Sepharose and subsequently analyzed by SDS−PAGE and immunoblotting using goat anti-FGF1 (Santa Cruz Biotechnology), mouse anti-myc (Upstate), or rabbit anti-FLAG (Cell Signaling Technology) antibodies. The purity of the fractions was verified using mouse anti-lamin A (Abcam), mouse anti-EGFR (BD Transduction Laboratories), rabbit anti-calreticulin (Stressgen), and rabbit anti-MAP kinase (p42/p44) (Cell Signaling Technology) antibodies.

Dynamic Light Scattering Measurements of Hydrodynamic Diameter. The hydrodynamic diameters of FGF1 wild type and FGF1 myc variants were measured by the dynamic light scattering system Zetasizer Nano ZS from Malvern Instruments Ltd. equipped with a 633 nm He−Ne laser and an avalanche photodiode detector. The calculated average hydrodynamic diameter resulted from three measurements of each sample made at 25 °C. The proteins were measured at a concentration of 1 mg/mL at pH 7.4.

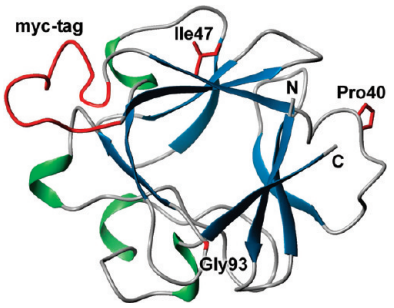

FIGURE 1: Model of FGF1 with the myc-tag loop insertion based on the 1rg8 FGF1 structure (*36*). β-Sheets are marked in blue, helices in green, and myc tag and mutations introduced to increase the stability of the growth factor in red color. The model was prepared with the program MOLMOL (*46*).

RESULTS

Construction and Production of FGF1 Fusion Proteins. Additional amino acids were inserted into FGF1 to test if the growth factor could carry heterologous polypeptides into the cytosol or the nucleus of FGF-receptor expressing cells. We previously observed that amino acids added to the terminal ends of FGF1 have the tendency to be cleaved off after endocytosis. We therefore decided to introduce amino acids inside the sequence of FGF1. We identified a surface loop in the three-dimensional structure of FGF1 that seemed to be suitable for insertion of additional amino acids (Figure 1). This loop is situated far from the regions in the FGF1 structure that are involved in binding to heparin and to specific FGF receptors. To make insertions with different lengths, we decided to introduce increasing number of copies of the myc tag. The polypeptides were inserted between valine 51 and glycine 52 in the FGF1 sequence. We constructed mutant FGF1 fusion proteins with the number of myc tags ranging from 1 to 13 (FGF1-myc1 (10 amino acids inserted), FGF1-myc2 (38 amino acids inserted), FGF1-myc3 (53 amino acids inserted), FGF1-myc5 (77 amino acids inserted), FGF1-myc8 (116 amino acids inserted), and FGF1-myc13 (181 amino acids inserted)).

We expressed the proteins in the *E. coli* BL21DE system and purified the FGF1 mutant proteins using a heparin−Sepharose column. All mutant proteins were expressed with a high yield (10−30 mg/L of culture) and bound to heparin with similar affinity as the wild-type FGF1.

Characterization of FGF1 Fusion Proteins. To elucidate how the introduction of an increasing number of copies of the myc tag into the FGF1 sequence affects the overall structure of the growth factor, we performed spectroscopic analysis. Conformation (secondary and tertiary structure) of the variants was verified by circular dichroism (CD) and fluorescence measurements.

The far-UV CD spectrum of the wild-type FGF1 shows a minimum at around 206 nm typical for β-sheet-rich proteins and a positive peak between 220 and 240 nm (with the maximum around 228 nm) resulting from β-turns, loops, and aromatic residues (*32*, *33*). When FGF1 is unfolded, due to the disruption of secondary structure, such a positive CD signal is replaced by a negative one. For all myc variants we observed differences in CD spectra as compared to the wild type (Figure 2A). Gradual lowering of the signal around 228 nm for the mutants suggested partial unfolding of FGF1 and loss of secondary structure upon

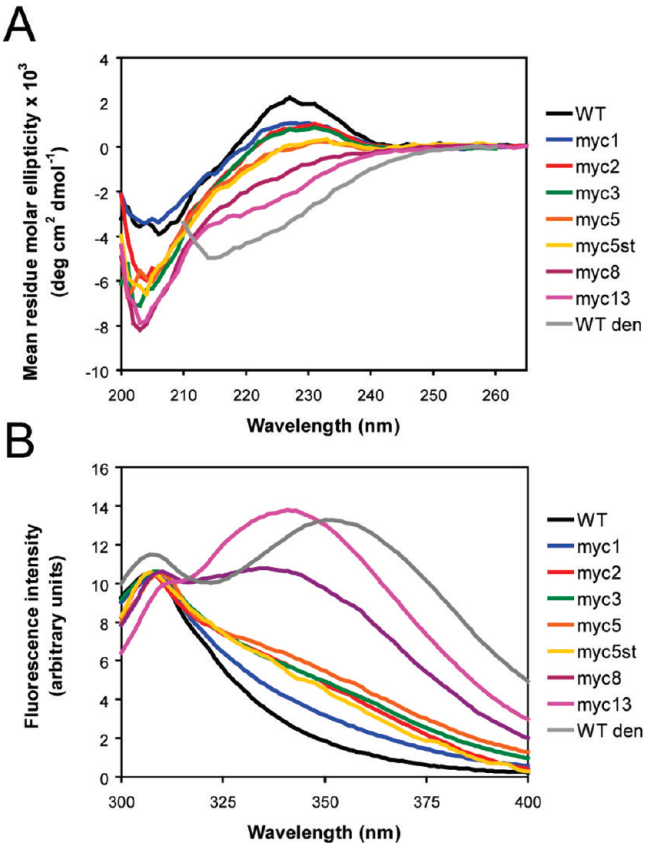

FIGURE 2: Spectroscopic characteristic of FGF1 wild type and myc variants. Far-UV circular dichroism spectra measured from 200 to 260 nm in a 1 cm cuvette (A) and fluorescence spectra measured from 300 to 400 nm in a 1 cm cuvette with excitation of 280 nm (B). WT den represents denatured FGF1 wild type.

extending its loop between residues 51 and 52. Spectra of the FGF1-myc8 and -myc13 revealed a negative signal between 220 and 240 nm and are more similar to the spectrum of denatured growth factor than to the wild type.

To ensure that the change in the ellipticity not only was caused by local relaxation of the structure but reflects the global unfolding of FGF1, we also measured the fluorescence spectra. The fluorescence spectrum of the properly folded wild-type FGF1 is dominated by multiple tyrosine fluorescence at approximately 305 nm. The signal from the single Trp (position 107) in native protein is completely quenched by proximal pyrrole and imidazole groups (*34*). However, when the tertiary structure is disrupted, the quenching effect is eliminated and the emission maximum is shifted to 350 nm characteristic for the indole side group of tryptophan. Thus, this wavelength can serve as a probe of native conformation of the growth factor. Fluorescence spectra of FGF1 variants containing different numbers of myc tags show that the longer the introduced sequence, the more unfolded the global structure of FGF1 (Figure 2B). However, a low number of myc epitopes caused slight unfolding of the FGF1 protein. FGF1-myc8 and -myc13 spectra show that the majority of protein molecules are transited into the unfolded fraction. The results show that the size of the loop determines how well the secondary and tertiary interactions are preserved.

We also tested how the introduction of various numbers of myc-tag sequences into the FGF1 molecule influenced the thermal stability of the growth factor (Figure 3, Supporting Information Results, and Supporting Information Figure S1). Analogically to the fluorescence and ellipticity spectra, it was

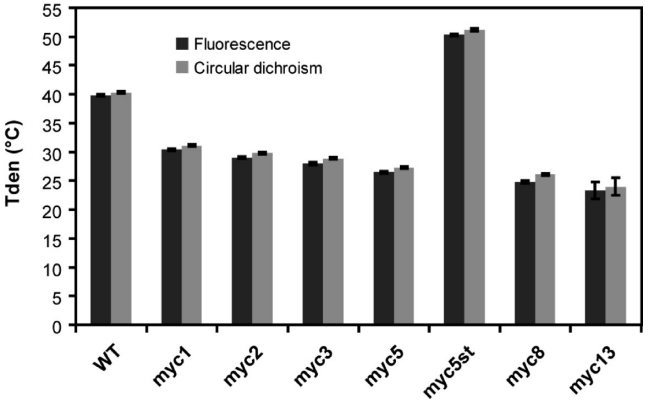

FIGURE 3: Thermodynamic stability of FGF1 mutants. The denaturation temperatures of the wild type and mutants monitored by fluorescence and circular dichroism in the presence of 0.7 M GdmCl. The data shown are mean values of three independent denaturation experiments ± standard error.

observed that addition of myc sequences decreased the stability of FGF1. Successive elongation of the FGF1 loop results in gradual lowering of the T_{den} value (Figure 3, Supporting Information Figure S1, and Supporting Information Table S1).

Since we observed that the larger myc variants revealed quite significant thermal destabilization compared to the wild type, we decided to construct a myc variant with increased thermodynamic stability. We took advantage of our previous observation that single amino acids substitutions in the FGF1 sequence considerably stabilize the growth factor (*29*). We used site-directed mutagenesis and introduced three stabilizing substitutions, Q40P, S47I, and H93G, in the sequence of the FGF1-myc5 construct (FGF1-myc5st) (Figure 1). These mutations strongly improved the stability of FGF1, increasing T_{den} of wild-type FGF1 from 40.3 to 61.8 °C ($\Delta T_{den} = 21.5$ °C) (*29*). We observed the same effect for the FGF1-myc5 variant. Although the three mutations did not change much the CD and fluorescence spectra of the FGF1-myc5 variant (Figure 2), they increased dramatically its thermal stability. The T_{den} of FGF1-myc5st was slightly above 50 °C and was over 23 °C higher than the T_{den} of FGF1-myc5 (Figure 3, Supporting Information Table S1). This result shows that the observed thermodynamic properties result from the additive effects of FGF1 molecule destabilization by myc sequences ($\Delta T_{den} = -13$ °C (Figure 3, Supporting Information Table S1)) and its stabilization by three point mutations.

To test whether the destabilizing effect of myc tags in the FGF1 loop can be compensated for by heparin, we performed thermal unfolding of FGF1 and myc variants in the presence or in the absence of this stabilizing polysaccharide. Heparin was found to stabilize effectively all tested variants, even to higher extent than the wild type with respect to denaturation temperature (Supporting Information Figure S2). In addition, these results confirm the proper binding of the FGF1 mutants to heparin.

Interaction of FGF1 Fusion Proteins with Cells Expressing FGFRs. In order to test if the mutant FGFs bind to specific FGF receptors and are endocytosed, we used confocal microscopy. We added the mutants to U2OS cells expressing FGFR1 and incubated the cells for 15 min to allow endocytosis to occur. After fixation, the cells were stained with antibodies against the myc tag and against the endosomal marker EEA1 to test if the FGF1 mutants were internalized into early endosomes. In all cases intracellular FGF1 myc variants (red dots) were observed,

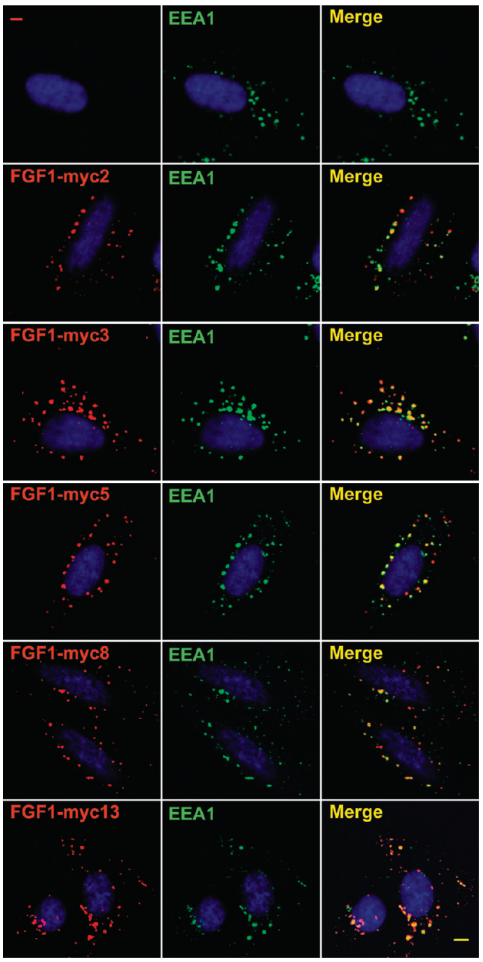

FIGURE 4: Binding and internalization of the FGF1 myc mutants. U2OS cells stably expressing FGFR1 were incubated with different FGF1 myc variants at 6.5 nM and 50 units/mL heparin at 37 °C for 15 min. The cells were then fixed and stained with anti-myc and anti-EEA1 antibodies and examined by confocal microscopy. Bar, 5 μm.

indicating that the mutants bound to cells expressing FGFR1 and that they were internalized into cells (Figure 4). We also observed extensive colocalization of the mutants with the marker of early endosomes, EEA1 (green dots), strongly suggesting that the mutants were internalized into early endosomes similarly to wild-type FGF1.

Next, we tested if the mutant proteins retained biological activity during long-term incubation with cells. For this purpose we applied a DNA synthesis stimulation assay. Increasing concentrations of wild-type FGF1 and the mutant proteins were added to serum-starved NIH/3T3 cells, and then the ability of the cells to incorporate radioactive thymidine was measured. Wild-type FGF1 stimulated DNA synthesis at a similar level as previously reported (*29*) (Figure 5). Stimulation started already at a growth factor concentration of 65 pM (equivalent to 1 ng/mL wild-type FGF1). The mutants were less active than wild-type FGF1 in this assay. Such behavior can be caused by the less rigid conformation of the mutants than of the wild type, which leads to their higher susceptibility to extracellular proteases and thermal unfolding during the long-term incubation. However, at 6.5 nM all of the mutants triggered a full cellular response with respect to stimulation of DNA synthesis. We therefore used this concentration when analyzing further the mutant FGFs.

To further characterize the interaction of the mutants with cells expressing FGFRs, we tested how the myc mutants activated

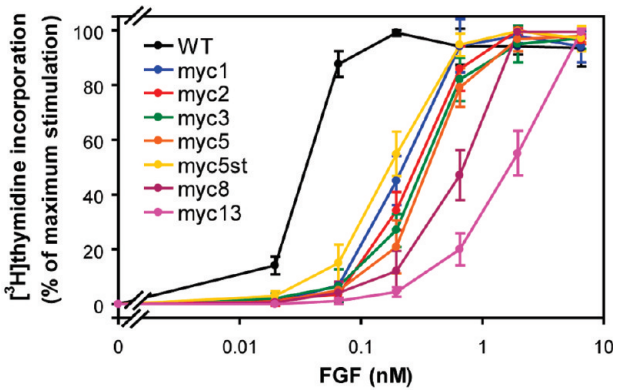

FIGURE 5: Mitogenic activity of wild-type and myc variants of FGF1. Normalized mitogenic activity curves derived from the [^{3}H]thymidine incorporation experiment in NIH/3T3 cells in the presence of 20 units/mL heparin. The data shown are mean values of four independent experiments ± SD.

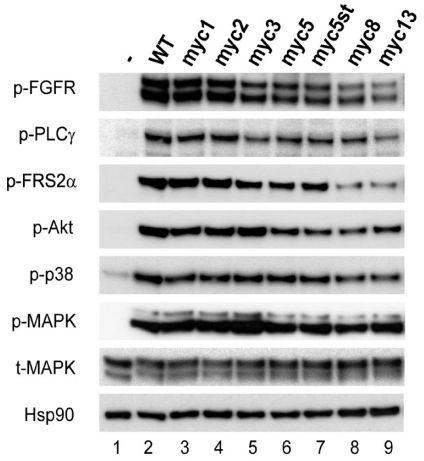

FIGURE 6: Ability of the wild-type and myc variants of FGF1 to activate signaling cascades after 15 min stimulation. Serum-starved NIH/3T3 cells were treated with 6.5 nM growth factor in the presence of 20 units/mL heparin. To assess the activation of the downstream proteins, anti-phosphoprotein antibodies were used. To verify equal loading, stripped membranes were blotted with antibodies that recognized the total amount of MAP kinases (t-MAPK) and Hsp90.

FGF receptors and downstream signaling cascades. Activation of the receptors was probed using antibodies recognizing the phosphorylated, active form of FGFR1 (Figure 6). In the absence of the growth factor there was no activation of the signaling pathways (lane 1). When wild-type FGF1 was added, there was a clear activation of the receptor (lane 2). Furthermore, we observed that all of the mutants were able to activate the receptor. However, the phosphorylation of the receptor became slightly weaker with the mutants with increasing number of myc tags. We used phospho-specific antibodies against several downstream signaling molecules to test further the ability of the mutants to activate FGF1 signaling pathways. As seen in Figure 6, the mutants activated all tested downstream signaling cascades, but to a slightly weaker extent than wild-type FGF1.

Taken together, the data show that the tested mutants are active, but an increasing number of myc tags in the FGF1 sequence evokes somewhat decreasing activities of the growth factor.

Translocation across Cellular Membranes. We then tested the ability of the mutants to translocate into cells. To investigate

the translocation of FGF1 from the cell surface to the cytosol and nucleus, we used a digitonin-based fractionation assay which was extensively described and validated in earlier studies by us and others (*9*, *12*, *17*, *20*, *35*). The mutants were added to NIH/3T3 cells for 6 h to allow the growth factors to be transported into the cells. Then, we fractionated the cells into membrane, cytosol, and nuclear fractions. We used digitonin to permeabilize the plasma membrane to allow cytosolic proteins to leak out. These proteins were recovered and called the cytosolic fraction. The remnants of the cells were lysed by Triton X-100 and fractionated by centrifugation into a membrane and a nuclear fraction.

As seen in Figure 7A (left panel, lane 2), wild-type FGF1 was found in all three fractions (membrane, cytosol, and nuclear). When bafilomycin A1, an inhibitor of the vesicular proton pump, was added together with FGF1, the translocation was blocked (lane 1) as reported before (*11*). FGF1 was then only found in the membrane fraction. In the absence of bafilomycin A1, the mutants FGF1-myc1, -myc2, and -myc3 were found in the cytosolic and the nuclear fraction (lanes 3, 4, and 5), indicating that they were efficiently translocated across the membrane into the cells. However, the mutants FGF1-myc5, -myc8, and -myc13 were only found in the membrane fraction, indicating that these mutants were not translocated across the membrane (lanes 6, 8, and 9). To verify the identity of the observed bands in the different fractions, we reprobed the Western blot membrane with anti-myc antibodies (Figure 7A, right panel). A similar pattern was then observed, showing that the protein bands represented indeed the added mutants. As expected, wild-type FGF1 was not detected when using myc antibodies since this protein did not contain the myc epitope (Figure 7A, right panel, lanes 1 and 2).

To affirm the quality of the fractionation procedure, we performed Western blotting with lysate from each fraction and incubated the membrane with antibodies against marker proteins for different compartments (Figure 7C). The EGF receptor (localized to cell-surface and endosomal membranes) and the endoplasmic reticulum protein calreticulin were both found in the membrane fraction and not in the cytosolic or nuclear fractions. The cytosolic proteins, the MAP kinases (MAPK), were only detected in the cytosol fraction, and the nuclear protein lamin A was only found in the nuclear fraction. We concluded that the procedure employed yielded adequate and pure fractions.

We were concerned that the decrease in stability observed for the mutants with inserted myc tags could be the cause of the lack of detectable translocation for the mutants with five or more myc tags. To test this possibility, we used the stabilized version of FGF1-myc5, the FGF1-myc5st. This mutant was more stable than FGF1-myc3 that was efficiently translocated. Importantly, the stabilized mutant of FGF1 as such (without the inserted myc tags) was translocated into cells as efficiently as the wild-type FGF1 (our unpublished results). As seen in Figure 7A (lane 7), even for the stabilized mutant FGF1-myc5st we could not detect any translocation.

The possibility existed that the differences in translocation between the mutants could be a cell-type specific feature. Hence, we performed the translocation experiment in another cell line. Using BJ cells we could observe the same size dependence for translocation of the mutants as in NIH/3T3 cells (Figure 7B).

The myc tag contains one lysine, which results in an increasing number of lysines in the multi-myc-tag mutants. Since ubiquitination of lysines can be a signal for degradation by the proteasome, we were concerned that the lack of the FGF1-myc5 in the cytosol and nucleus could be due to increased proteasomal

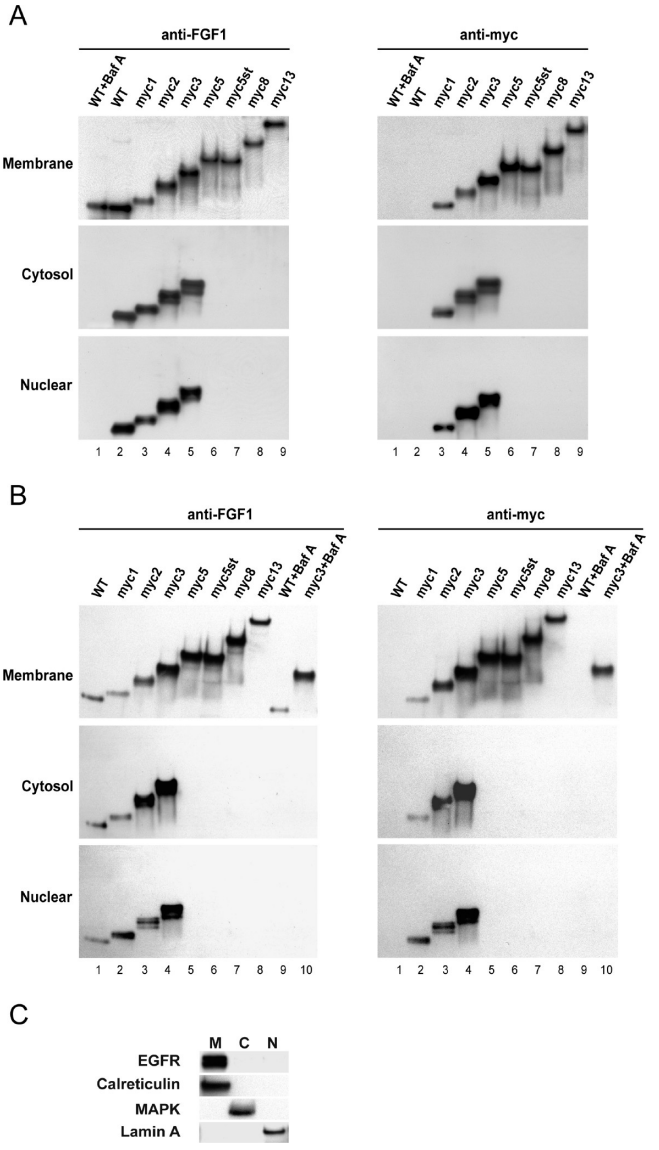

FIGURE 7: Translocation of wild-type and myc variants of FGF1 to cytosol and nucleus. NIH/3T3 cells (A) and BJ cells (B) were incubated with 6.5 nM FGF1 (WT) or FGF1 myc variants in the presence of 20 units/mL heparin for 6 h. The cells were fractionated into membrane, cytosolic, and nuclear fractions. FGF1 or FGF1 myc mutants were extracted from each fraction by binding to heparin−Sepharose and analyzed by SDS−PAGE and immunoblotting using anti-myc or anti-FGF1 antibodies. In some cases, 10 nM bafilomycin A1 (Baf A) was added. The cytosol and nuclear fractions were exposed to film for twice as long as the membrane fraction. (C) Lysates from each fraction (M, membrane; C, cytosol; N, nuclear) were analyzed by SDS−PAGE and immunoblotting using antibodies against the EGF receptor (EGFR), calreticulin, MAPK, and lamin A.

degradation and not because of blocked translocation. To test this possibility, we performed translocation experiments with FGF1, FGF1-myc3, and FGF1-myc5 in the presence of the proteasomal inhibitor, lactacystin (Figure 8). In the presence of lactacystin we could still not observe any band in the cytosolic or nuclear fraction for FGF1-myc5 (lane 6). Interestingly, for the wild-type FGF1 and FGF1-myc3 which both were translocated, the intensity of the bands increased slightly in the nuclear fraction (lanes 2 and 4), indicating that FGF1 is to some extent degraded by proteasomes after translocation into the nucleus. However, as no band appeared for the FGF1-myc5 mutant in the presence of

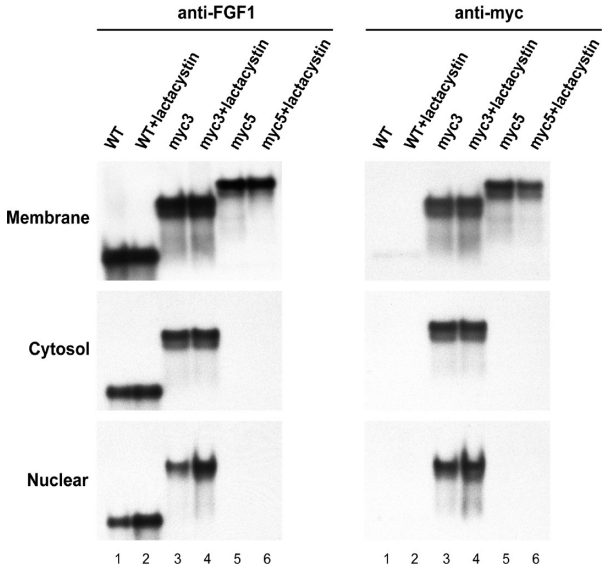

FIGURE 8: Effect of lactacystin on observed growth factor translocation. BJ cells were treated with 6.5 nM FGF1 (WT), FGF1-myc3, or FGF1-myc5 in the presence of 20 units/mL heparin for 6 h, with or without 10 μM lactacystin, and examined as in Figure 7. The left panel was treated with anti-FGF1 antibodies. The right panel shows the same immunoblot stripped and incubated with anti-myc antibodies.

proteasomal inhibitor, it seems clear that this mutant was not translocated into the cell at all.

We also considered the possibility that the observed translocation of the fusion proteins could be related to the properties of the inserted amino acids. To test this, we constructed other mutants containing unrelated sequences inside the same loop in FGF1 as the myc tags. We constructed one mutant fusion protein where we inserted the 3×FLAG tag (three copies of the FLAG tag) consisting of 22 amino acids and another variant containing the streptavidin binding peptide (SBP, 50 amino acids). As seen in Figure 9A,B, these mutants were translocated into the cytosol and nucleus similarly to the wild-type FGF1. Thus, different, unrelated sequences can be added to FGF1 and efficiently translocated into the cytosol and nucleus.

The translocation experiments using myc-tag mutants of FGF1 showed that inserts containing 77 amino acids (five myc tags) or more were not translocated. To test whether the block in translocation was unique to the multi-myc-tag variants (five myc tags or more), we made two additional fusion proteins with larger inserts. In one construct, we inserted the calmodulin binding peptide (CBP) together with the SBP tag (FGF1-SBP-CBP, 82 amino acids inserted). In another, we inserted the A-chain from the ricin toxin (FGF1-RTA, 272 amino acids inserted). We then tested if they were translocated into cells. Similarly to mutants with five or more myc tags, these fusion proteins with inserts larger than 77 amino aicds were not translocated into the cytosol or nucleus of BJ cells (Figure 9C).

Finally, we wanted to estimate the size of the putative FGF1 translocation pore. We previously showed that FGF1 translocates across the membrane in a folded form (*18*). Thus, by measuring the globular size of the translocated and nontranslocated mutants, we had the possibility to estimate the diameter of the translocation pore. In order to refine the estimation, we constructed an additional mutant, the FGF1-myc4 which has 67 amino acids inserted. We performed a translocation experiment comparing FGF1-myc3, -myc4, and -myc5. As can be seen in Figure 9D, FGF1-myc3 was translocated, while FGF1-myc4 translocation was severely reduced. In order to observe bands for FGF1-myc4 in the cytosol and nucleus, the Western blot membrane was exposed for an extended time period. FGF1-myc5 was not translocated at all as shown above. We then attempted to measure the actual globular size of the mutants. For this purpose, we used dynamic light scattering to measure the hydrodynamic diameter of the constructs. First, we measured the diameter of wild-type FGF1 to be 4.0 nm, corresponding exactly to the size of the FGF1 from the crystal structure (*36*). As a control, we measured the hydrodynamic diameter of lysozyme. We obtained a diameter of 3.7 nm, which is similar to previously published results where the size was shown to be 3.72 (*37*). We then measured the diameter of the myc variants and obtained the following results: FGF1-myc3, 5.0 nm; FGF1-myc4, 5.4 nm; FGF1-myc5, 6.6 nm. Thus as expected, increasing the length of the insert results in a larger globular size. As the translocation of FGF1-myc4 was severely reduced, we estimate the pore size to be between 5 and 6 nm.

We conclude that FGF1 can bring peptides of different lengths into cells, but there is a limitation on the number of amino acids that can be imported due to a restricted pore size.

DISCUSSION

In the present paper we provided evidence that FGF1 can deliver heterologous polypeptides into the cytosol and nucleus of mammalian cells. However, we also showed that there is a size limitation in the translocation of FGF1 fusion proteins across the cellular membrane. It was possible to insert approximately 50 amino acids into FGF1 and still observe translocation to the cytosol and nucleus. Inserting more residues (77 amino acids) blocked translocation completely. We clearly showed that the addition of amino acids in the surface loop of the FGF1 molecule increased the globular size of the growth factor. As FGF1 appears to be translocated across the membrane in a folded form (*18*), the fusion proteins with a higher number of myc tags (five myc tags or more) become too big to be translocated across the membrane. This implies that FGF1 is most probably translocated through a defined pore and not simply through leakage from ruptured membranes.

The efficiency of translocation seems to be identical for the mutants FGF1-myc1, -myc2, and -myc3 and wild-type FGF1, while there is a complete block in translocation when the mutants with five myc tags or more are added to the cells (see Figure 7). This indicates that the size of the translocation pore is strictly defined and that the passage is only possible for substrates with a size smaller than the exclusion limit, here defined by the FGF1 fusion proteins. Interestingly, both FGF2 and Tat proteins are smaller than the FGF1-myc3 mutant. We were able to estimate the actual size of the translocation pore by measuring the diameter of the multi-myc variants by dynamic light scattering. The pore seems to have a diameter of 5−6 nm, which is similar to what has been observed for another protein translocation pore, the Sec61 translocon (estimated to be between 4 and 6 nm (*38*)).

We attempted to visualize FGF1-myc3 in the nucleus by immunofluorescence using anti-myc antibodies. Unfortunately, we were not able to convincingly detect the fusion protein in the nucleus even if the construct was readily observed in endosomes. The growth factor is in this case concentrated in the relatively small endosomal volume resulting in a high signal. In the nucleus the growth factor is probably more diffused due to the large

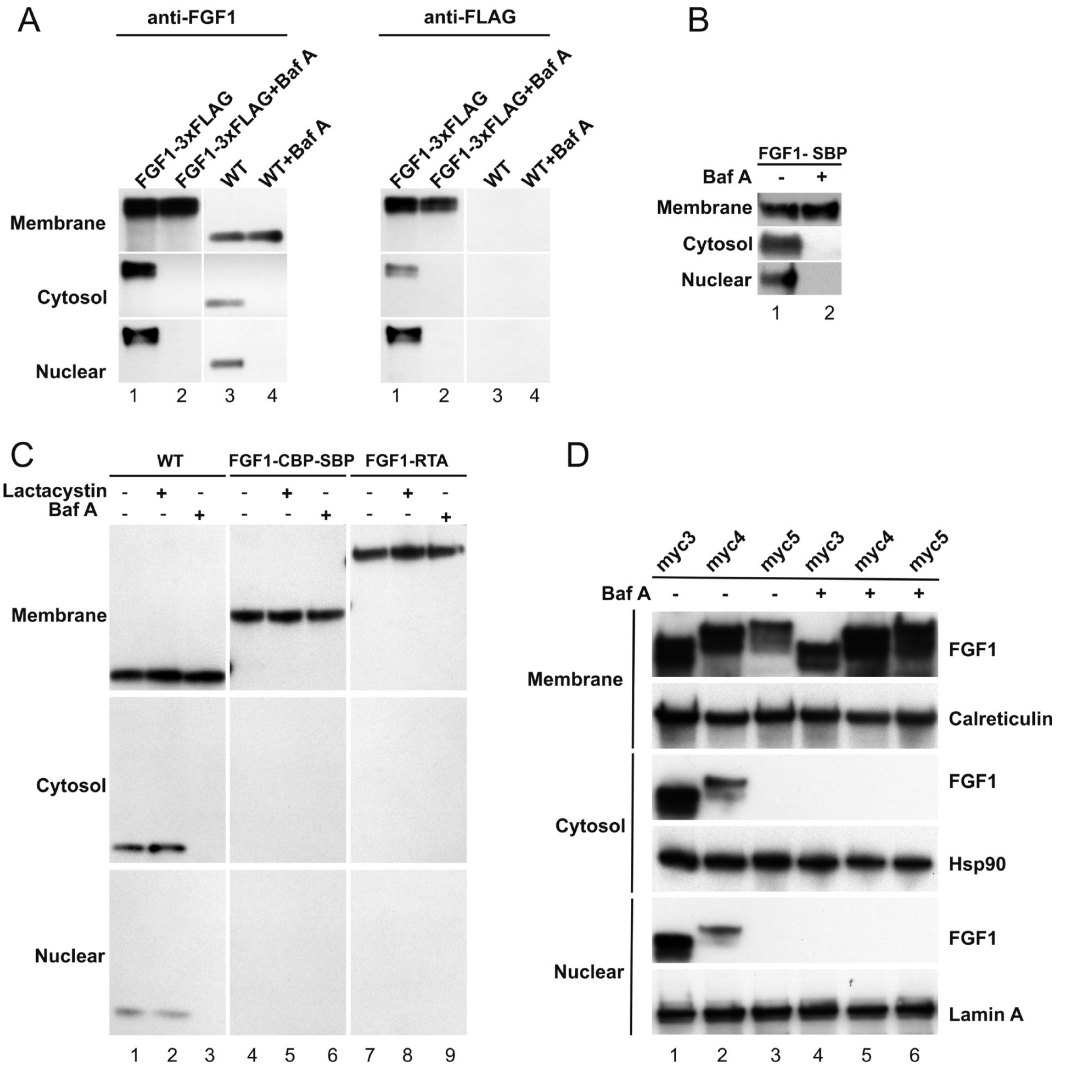

FIGURE 9: Translocation of various FGF1 fusion proteins. (A) BJ cells were treated with 6.5 nM FGF1-3×FLAG and FGF1 wild type (WT) in the presence of 20 units/mL heparin for 6 h and examined as in Figure 7. The left panel was treated with anti-FGF1 antibodies. The right panel shows the same immunoblot stripped and incubated with anti-FLAG antibodies. In some cases, 10 nM bafilomycin A1 (Baf A) was added. (B) BJ cells were incubated with FGF1-SBP for 6 h in the presence of 20 units/mL heparin and analyzed as in Figure 7. In one case, 10 nM bafilomycin A1 (Baf A) was added. (C) BJ cells were incubated with FGF1-CBP-SBP and FGF1-RTA for 6 h in the presence of 20 units/mL heparin and analyzed as in Figure 7. In some cases, 10 μM lactacystin or 10 nM bafilomycin A1 (Baf A) was added. (D) BJ cells were incubated with FGF1-myc3, -myc4, and -myc5 for 6 h in the presence of 20 units/mL heparin. The cells were fractionated and analyzed as in Figure 7. Cells analyzed in lanes 4−6 were incubated with 10 nM bafilomycin A1. Antibodies against marker proteins for each fraction were used as a control for equal loading (anti-calreticulin, anti-hsp90, and anti-lamin A).

nuclear volume and does not produce a detectable signal. However, the constructs with several myc tags can be useful for the study of endocytosis and endosomal transport as they considerably increase the signal in immunofluorescence.

We used the three-dimensional crystal structure of FGF1 to determine where to introduce the inserted polypeptides. We carefully chose a loop in the FGF1 molecule that was situated away from the regions involved in binding to the FGF receptors and to heparin. Indeed, the mutants bound to both heparin and to FGF receptors similarly to the wild type. Nevertheless, the observed activities of the mutants were somewhat reduced (see Figure 5). It is possible that the introduced polypeptides interfered with the formation of the complex between the ligand, the receptor, and heparin. The steric hindrance of the inserted amino acids could make this complex more unstable, leading to reduced activity. However, a more likely explanation of this effect is the impact of the extended loop on the stability of the mutants as such (see Figures 2 and 3). Introduction of additional amino acids into the structure could disturb the proper folding and make the protein less rigid and prone to proteolysis. During long-term signaling required for the stimulation of DNA synthesis, these effects may become more detectable (*15*). However, the lower activity of the mutants could be compensated for by the addition of a higher concentration of the growth factors (6.5 nM).

Although we used high concentrations of the growth factors in translocation experiments, we were concerned that the lower stability of the mutants could cause the lack of detection of translocated FGF1-myc5 and larger mutants in the cytosol and nucleus. To test this, we constructed a stabilized version of FGF1-myc5, the FGF1-myc5st mutant. We found that the mutant, even if it was more thermodynamically stable than the translocating mutant FGF1-myc3, still did not translocate. These results indicate that it is the size and not the reduced stability of the mutants that is the reason for the block in translocation.

To test if the myc sequences as such could influence the translocation, we constructed other FGF1 mutants containing

completely unrelated polypeptides. The mutants with smaller insertions (22 and 50 amino acids) were translocated efficiently into the cytosol and nucleus of cells, while the insertion of larger polypeptides (82 and 272 amino acids) resulted in no translocation. Furthermore, there was a possibility that the net charge of the inserts could influence translocation of the fusion proteins. In fact, the myc tag possesses several negatively charged amino acids which increase the net negative charge in the multi-myc-tag constructs. The myc3 insert has a charge of −9, myc4 of −12, and myc5 of −16. However, the other nontranslocating mutant, FGF1-SBP-CBP with a size of the insert similar to myc5, has a positive charge of 8. Thus, there is no correlation between charge and translocation. We therefore believe that it is the FGF1 sequence solely and not the amino acid composition of the insert that dictates if the fusion protein is translocated or not as long as the size of the whole molecule is small enough to fit into the translocation pore.

FGF1 has been shown to bind to intracellular chaperones, Hsp90 and Grp75, which are possibly involved in its translocation across the membrane (*17*, *39*). It is not clear how these proteins are involved in mediating translocation, but one can speculate that a reduced interaction between a chaperone and the larger constructs could be the reason for their failure in translocation. This hypothesis requires further investigation into the role of the chaperones in translocation before it could be clarified.

It has been proposed that nuclear FGF1 may be involved in the regulation of DNA synthesis (*4*, *5*). If FGF1 acts directly in inducing replication, a difference in DNA synthesis between the translocating and nontranslocating mutants could be expected. However, the observed difference between myc3 and myc5 in DNA synthesis experiments is small. It seems that, at least in NIH/3T3 cells, FGF1 does not influence directly the induction of DNA synthesis. We speculate that FGF1 may act indirectly in the nucleus of cells by, for instance, having an anti-apoptotic/pro-survival role, thereby increasing the number of cells that undergo mitosis and increasing the total measured DNA synthesis in a cell population.

An interesting implication of this work is the possibility of using the FGF1 translocation pathway to import polypeptides into the cytosol to induce MHC class I immunity (*40*). Another possible application is to use FGF1 as a carrier of toxic polypeptides acting in the cytosol or nucleus. Such constructs could be used to kill specifically cancer cells overexpressing FGFRs on the cell surface, providing a targeted therapy approach to tumors depending on FGFR signaling. Overexpression of FGFRs has been identified in several cancers, i.e., bladder, prostate, and breast cancers (*41*−*43*).

It is fascinating that there exists a pathway for translocation of proteins from endosomes into the cytosol and nucleus. The presented data argue that there might be a pore or a channel for FGF1 of some sort similarly to other membrane translocation systems (*44*, *45*) and that there is a strict size limitation for the translocation.

ACKNOWLEDGMENT

We are grateful to Anne Gro Bredesen and Hanne Guldsten for expert technical assistance and to Dr. Ken Rosendal for three-dimensional structure analysis. The authors are grateful to Dr. Daniel Krowarsch for help in preparation of figures.

SUPPORTING INFORMATION AVAILABLE

Thermodynamic parameters for the thermal denaturation of wild-type and myc mutants of FGF1 monitored by fluorescence and circular dichroism (Table S1), normalized thermal denaturation curves of FGF1 and its variants (Figure S1), and thermal denaturation curves of FGF1 and its variants in the presence and absence of heparin (Figure S2). This material is available free of charge via the Internet at http://pubs.acs.org.

REFERENCES

1. Schlessinger, J. (2004) Common and distinct elements in cellular signaling via EGF and FGF receptors. *Science 306*, 1506–1507.
2. Haugsten, E. M., Sorensen, V., Brech, A., Olsnes, S., and Wesche, J. (2005) Different intracellular trafficking of FGF1 endocytosed by the four homologous FGF receptors. *J. Cell Sci. 118*, 3869–3881.
3. Haugsten, E. M., Malecki, J., Bjorklund, S. M., Olsnes, S., and Wesche, J. (2008) Ubiquitination of fibroblast growth factor receptor 1 is required for its intracellular sorting but not for its endocytosis. *Mol. Biol. Cell 19*, 3390–3403.
4. Imamura, T., Engleka, K., Zhan, X., Tokita, Y., Forough, R., Roeder, D., Jackson, A., Maier, J. A., Hla, T., and Maciag, T. (1990) Recovery of mitogenic activity of a growth factor mutant with a nuclear translocation sequence. *Science 249*, 1567–1570.
5. Wiedlocha, A., Falnes, P. O., Madshus, I. H., Sandvig, K., and Olsnes, S. (1994) Dual mode of signal transduction by externally added acidic fibroblast growth factor. *Cell 76*, 1039–1051.
6. Kolpakova, E., Wiedlocha, A., Stenmark, H., Klingenberg O., Falnes, P. O., and Olsnes, S. (1998) Cloning of an intracellular protein that binds selectively to mitogenic acidic fibroblast growth factor. *Biochem. J. 336* (Part 1), 213–222.
7. Skjerpen, C. S., Nilsen, T., Wesche, J., and Olsnes, S. (2002) Binding of FGF-1 variants to protein kinase CK2 correlates with mitogenicity. *EMBO J. 21*, 4058–4069.
8. Skjerpen, C. S., Wesche, J., and Olsnes, S. (2002) Identification of ribosome-binding protein p34 as an intracellular protein that binds acidic fibroblast growth factor. *J. Biol. Chem. 277*, 23864–23871.
9. Sorensen, V., Zhen, Y., Zakrzewska, M., Haugsten, E. M., Walchli, S., Nilsen, T., Olsnes, S., and Wiedlocha, A. (2008) Phosphorylation of fibroblast growth factor (FGF) receptor 1 at Ser777 by p38 mitogen-activated protein kinase regulates translocation of exogenous FGF1 to the cytosol and nucleus. *Mol. Cell. Biol. 28*, 4129–4141.
10. Sorensen, V., Wiedlocha, A., Haugsten, E. M., Khnykin, D., Wesche, J., and Olsnes, S. (2006) Different abilities of the four FGFRs to mediate FGF-1 translocation are linked to differences in the receptor C-terminal tail. *J. Cell Sci. 119*, 4332–4341.
11. Malecki, J., Wiedlocha, A., Wesche, J., and Olsnes, S. (2002) Vesicle transmembrane potential is required for translocation to the cytosol of externally added FGF-1. *EMBO J. 21*, 4480–4490.
12. Wesche, J., Malecki, J., Wiedlocha, A., Ehsani, M., Marcinkowska, E., Nilsen, T., and Olsnes, S. (2005) Two nuclear localization signals required for transport from the cytosol to the nucleus of externally added FGF-1 translocated into cells. *Biochemistry 44*, 6071–6081.
13. Wiedlocha, A., Falnes, P. O., Rapak, A., Munoz, R., Klingenberg, O., and Olsnes, S. (1996) Stimulation of proliferation of a human osteosarcoma cell line by exogenous acidic fibroblast growth factor requires both activation of receptor tyrosine kinase and growth factor internalization. *Mol. Cell. Biol. 16*, 270–280.
14. Malecki, J., Wesche, J., Skjerpen, C. S., Wiedlocha, A., and Olsnes, S. (2004) Translocation of FGF-1 and FGF-2 across vesicular membranes occurs during G1-phase by a common mechanism. *Mol. Biol. Cell 15*, 801–814.
15. Zhan, X., Hu, X., Friesel, R., and Maciag, T. (1993) Long term growth factor exposure and differential tyrosine phosphorylation are required for DNA synthesis in BALB/c 3T3 cells. *J. Biol. Chem. 268*, 9611–9620.
16. Klingenberg, O., Wiedlocha, A., Rapak, A., Khnykin, D., Citores, L., and Olsnes, S. (2000) Requirement for C-terminal end of fibroblast growth factor receptor 4 in translocation of acidic fibroblast growth factor to cytosol and nucleus. *J. Cell Sci. 113*, 1827–1838.
17. Wesche, J., Malecki, J., Wiedlocha, A., Skjerpen, C. S., Claus, P., and Olsnes, S. (2006) FGF-1 and FGF-2 require the cytosolic chaperone Hsp90 for translocation into the cytosol and the cell nucleus. *J. Biol. Chem. 281*, 11405–11412.
18. Wesche, J., Wiedlocha, A., Falnes, P. O., Choe, S., and Olsnes, S. (2000) Externally added aFGF mutants do not require extensive

unfolding for transport to the cytosol and the nucleus in NIH/3T3 cells. *Biochemistry 39*, 15091–15100.
19. Klingenberg, O., Wiedlocha, A., Citores, L., and Olsnes, S. (2000) Requirement of phosphatidylinositol 3-kinase activity for translocation of exogenous aFGF to the cytosol and nucleus. *J. Biol. Chem. 275*, 11972–11980.
20. Wiedlocha, A., Nilsen, T., Wesche, J., Sorensen, V., Malecki J., Marcinkowska, E., and Olsnes, S. (2005) Phosphorylation-regulated nucleocytoplasmic trafficking of internalized fibroblast growth factor-1. *Mol. Biol. Cell 16*, 794–810.
21. Nilsen, T., Rosendal, K. R., Sorensen, V., Wesche, J., Olsnes, S., and Wiedlocha, A. (2007) A nuclear export sequence located on a beta-strand in fibroblast growth factor-1. *J. Biol. Chem. 282*, 26245–26256.
22. Baldin, V., Roman, A. M., Bosc-Bierne, I., Amalric, F., and Bouche, G. (1990) Translocation of bFGF to the nucleus is G1 phase cell cycle specific in bovine aortic endothelial cells. *EMBO J. 9*, 1511–1517.
23. Claus, P., Doring, F., Gringel, S., Muller-Ostermeyer, F., Fuhlrott J., Kraft, T., and Grothe, C. (2003) Differential intranuclear localization of fibroblast growth factor-2 isoforms and specific interaction with the survival of motoneuron protein. *J. Biol. Chem. 278*, 479–485.
24. Gringel, S., van, B. J., Haastert, K., Grothe, C., and Claus, P. (2004) Nuclear fibroblast growth factor-2 interacts specifically with splicing factor SF3a66. *Biol. Chem. 385*, 1203–1208.
25. Ma, X., Dang, X., Claus, P., Hirst, C., Fandrich, R. R., Jin, Y., Grothe, C., Kirshenbaum, L. A., Cattini, P. A., and Kardami, E. (2007) Chromatin compaction and cell death by high molecular weight FGF-2 depend on its nuclear localization, intracrine ERK activation, and engagement of mitochondria. *J. Cell Physiol. 213*, 690–698.
26. Vendeville, A., Rayne, F., Bonhoure, A., Bettache, N., Montcourrier, P., and Beaumelle, B. (2004) HIV-1 Tat enters T cells using coated pits before translocating from acidified endosomes and eliciting biological responses. *Mol. Biol. Cell 15*, 2347–2360.
27. Frankel, A. D., and Pabo, C. O. (1988) Cellular uptake of the tat protein from human immunodeficiency virus. *Cell 55*, 1189–1193.
28. Gimenez-Gallego, G., Conn, G., Hatcher, V. B., and Thomas, K. A. (1986) The complete amino acid sequence of human brain-derived acidic fibroblast growth factor. *Biochem. Biophys. Res. Commun. 138*, 611–617.
29. Zakrzewska, M., Krowarsch, D., Wiedlocha, A., Olsnes, S., and Otlewski, J. (2005) Highly stable mutants of human fibroblast growth factor-1 exhibit prolonged biological action. *J. Mol. Biol. 352*, 860–875.
30. Blaber, S. I., Culajay, J. F., Khurana, A., and Blaber, M. (1999) Reversible thermal denaturation of human FGF-1 induced by low concentrations of guanidine hydrochloride. *Biophys. J. 77*, 470–477.
31. Zakrzewska, M., Krowarsch, D., Wiedlocha, A., and Otlewski, J. (2004) Design of fully active FGF-1 variants with increased stability. *Protein Eng., Des. Sel. 17*, 603–611.
32. Mach, H., Ryan, J. A., Burke, C. J., Volkin, D. B., and Middaugh C. R. (1993) Partially structured self-associating states of acidic fibroblast growth factor. *Biochemistry 32*, 7703–7711.
33. Srimathi, T., Kumar, T. K., Kathir, K. M., Chi, Y. H., Srisailam S., Lin, W. Y., Chiu, I. M., and Yu, C. (2003) Structurally homologous all beta-barrel proteins adopt different mechanisms of folding. *Biophys. J. 85*, 459–472.
34. Copeland, R. A., Ji, H., Halfpenny, A. J., Williams, R. W., Thompson, K. C., Herber, W. K., Thomas, K. A., Bruner, M. W., Ryan, J. A., and Marquis-Omer, D.; et al. (1991) The structure of human acidic fibroblast growth factor and its interaction with heparin. *Arch. Biochem. Biophys. 289*, 53–61.
35. Heine, K., Pust, S., Enzenmuller, S., and Barth, H. (2008) ADP-ribosylation of actin by the *Clostridium botulinum* C2 toxin in mammalian cells results in delayed caspase-dependent apoptotic cell death. *Infect. Immun. 76*, 4600–4608.
36. Bernett, M. J., Somasundaram, T., and Blaber, M. (2004) An atomic resolution structure for human fibroblast growth factor 1. *Proteins 57*, 626–634.
37. Grigsby, J. J., Blanch, H. W., and Prausnitz, J. M. (2000) Diffusivities of lysozyme in aqueous $MgCl_2$ solutions from dynamic light-scattering data: effect of protein and salt concentrations. *J. Phys. Chem. B 104*, 3645–3650.
38. Hamman, B. D., Chen, J. C., Johnson, E. E., and Johnson, A. E. (1997) The aqueous pore through the translocon has a diameter of 40−60 Å during cotranslational protein translocation at the ER membrane. *Cell 89*, 535–544.
39. Mizukoshi, E., Suzuki, M., Loupatov, A., Uruno, T., Hayashi H., Misono, T., Kaul, S. C., Wadhwa, R., and Imamura, T. (1999) Fibroblast growth factor-1 interacts with the glucose-regulated protein GRP75/mortalin. *Biochem. J. 343* (Part 2), 461–466.
40. Doling, A. M., Ballard, J. D., Shen, H., Krishna, K. M., Ahmed R., Collier, R. J., and Starnbach, M. N. (1999) Cytotoxic T-lymphocyte epitopes fused to anthrax toxin induce protective antiviral immunity. *Infect. Immun. 67*, 3290–3296.
41. Knowles, M. A. (2008) Novel therapeutic targets in bladder cancer: mutation and expression of FGF receptors. *Future Oncol. 4*, 71–83.
42. Chin, K., DeVries, S., Fridlyand, J., Spellman, P. T., Roydasgupta, R., Kuo, W. L., Lapuk, A., Neve, R. M., Qian, Z., Ryder, T., Chen, F., Feiler, H., Tokuyasu, T., Kingsley, C., Dairkee, S., Meng, Z., Chew, K., Pinkel, D., Jain, A., Ljung, B. M., Esserman, L., Albertson, D. G., Waldman, F. M., and Gray, J. W. (2006) Genomic and transcriptional aberrations linked to breast cancer pathophysiologies. *Cancer Cell 10*, 529–541.
43. Gowardhan, B., Douglas, D. A., Mathers, M. E., McKie, A. B., McCracken, S. R., Robson, C. N., and Leung, H. Y. (2005) Evaluation of the fibroblast growth factor system as a potential target for therapy in human prostate cancer. *Br. J. Cancer 92*, 320–327.
44. Schatz, G., and Dobberstein, B. (1996) Common principles of protein translocation across membranes. *Science 271*, 1519–1526.
45. Matlack, K. E., Mothes, W., and Rapoport, T. A. (1998) Protein translocation: tunnel vision. *Cell 92*, 381–390.
46. Koradi, R., Billeter, M., and Wuthrich, K. (1996) MOLMOL: a program for display and analysis of macromolecular structures. *J. Mol. Graphics 14*, 51–32.